

The Role of Coalescence in Inkjet Printing Functional Films: An Experimental Study

J. William Boley, ChenChao Shou, Patrick McCarthy, Timothy Fisher, and George T.C.-Chiu; Purdue University; West Lafayette, IN/USA

Abstract

For the past several decades inkjet technology has been shown to be a useful tool for fabricating anything from three dimensional objects to electrical devices and biological sensors. From a manufacturing perspective, it is important to functionalize a substrate with material in as timely a manner as possible while maintaining optimal functionality and satisfying hardware limitations. Of particular interest in previous work has been the effect of drop coalescence on print quality. This work examines how coalescence affects the uniformity of printed pairs of drops and printed lines as well as the functional performance of printed lines of a Pd based ink on Silicon and oxidized Silicon substrates. The results indicate that the ink migration resulting from Marangoni flows can be minimized by avoiding coalescence of adjacently deposited drops, thus increasing film uniformity and improving functional performance.

Introduction

For more than a decade inkjet technology has been proven to be a useful fabrication tool for functionally print electronics [1–7], sensors [1, 7, 8], three dimensional objects [8, 9], and biological materials [1, 7, 10]. Coalescence of adjacently located drops on a non-porous substrate is one key physical phenomenon of the deposition process that has received attention from several researchers [11–18] due to its direct effect on functional performance.

Coalescence and Functional Inkjet Print Quality

Most studies in the literature on functional inkjet printing have adopted methods of coalescing adjacently printed drops [1–5, 7, 9–12, 19]. Two widely used approaches for inkjet printing coalesced films are the works of Stringer and Derby [11] and the works of Soltman et al. [12].

Stringer and Derby [11] used a conservation of volume model proposed by Duineveld [20] to obtain a minimum drop spacing that guarantees stability of printed coalesced lines (i.e. that the coalesced bead will maintain a contact angle between its advanced and receding contact angles) for an arbitrary ink-substrate combination, assuming that the contact line remains pinned and evaporation is negligible. The test bed they used consisted of two inks (a silver nanoparticle ink and an in-house organometallic salt dissolved in xylene) and three substrates (glass, polyimide, and silicone). Their results agreed well with their predictions for the silver nanoparticle ink. However, they found discrepancies with

the organometallic salt dissolved in xylene, which was attributed to the high vapor pressure of xylene and the fact that the Duineveld model assumed negligible evaporation between the deposition times of the consecutively printed drops.

Soltman et al. [12] extended coalesced partially wetting films to printed rectangles. In their work they proposed a print routine that held a fixed drop spacing within a printed row and proposed a variable drop spacing between printed rows. The drop spacing between rows was calculated based on an evaporation model proposed by Hu and Larson [21]. Applying their approach to an ink-substrate system of poly-4-vinylphenol, a low vapor pressure ink used in printed dielectrics, on glass resulted in improved rectangular edge definition. However, the coalesced films exhibited the coffee ring effect (the accumulation of functional particles on the drop boundary caused by capillary flow during evaporation [22]) at the scale of the entire film, thus requiring additional tuning of the ink by solvent mixing [23] or particle shaping [24] in order to guarantee uniform films.

A less popular method of functional inkjet printing is to avoid the occurrence of coalescence altogether. This approach was followed by Boley et al. [6, 13] for two types of ink (an in-house Pd thiolate dissolved in toluene (Pd ink) and an in-house suspension of single-walled carbon nanotubes synthesized with single strand deoxyribonucleic acid (ssDNA-SWCNT ink)) onto oxidized silicon wafers with printed electronics as the application. This two-pass approach consisted of printing every other pixel within each line on the first pass, avoiding touching of liquid drops. Allowing time for the solvent to evaporate from the drops printed on the first pass, the print-head returned to the beginning of the line for the second pass and deposited ink onto the remaining pixels. Figure 1 shows the building of a multi-layered line. Printing the additional layers benefits the functional performance by making the cross section of the line more uniform and by increasing the amount of functional material per unit length, thereby decreasing the sheet resistance. As can be seen from Figure 1, the additional layers do not significantly change the line width.

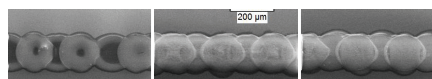


Figure 1. Sequence of SEM images depicting the construction of a multi-layer line segment printed using a two pass print mode. (Left) One layer. (Middle) Three layers. (Right) Five layers.

The lines printed by this method were quite uniform. Additional images of the printed lines were captured after burning off the

organic matter to observe any effects of the thermolysis step on the continuity of the lines. As evident from Figure 2, the uniformity and continuity of the printed lines remained unchanged after thermolysis.

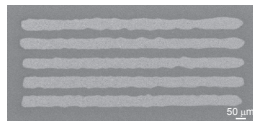


Figure 2. Post-thermolysis SEM image of five five-layer printed line segments of a 300mM solution of Pd hexadecanethiolate in toluene.

In order to characterize functional performance, additional experiments were conducted to print five-layer four probe patterns of Pd ink at different concentrations with different chain lengths. From the known geometry of the pattern, the resistivity was found to be $(4.6 \pm 0.8) \times 10^{-6} \Omega\text{m}$ for traces derived from the hexadecanethiolate precursor and $(2.5 \pm 0.4) \times 10^{-6} \Omega\text{m}$ for those from the butanethiolate, a result competitive with e-beam fabricated patterns involving Pd [6].

In the same studies, the authors extended their work to include inkjet printed networks of SWCNTs. In the authors demonstration experiments, a network of SWCNTs was formed by printing two layers of an aqueous solution of SWCNTs wrapped with single-stranded DNA (SSDNA) using the same two pass print mode for the printed Pd patterns. The technique developed to disperse SWCNTs with SSDNA in aqueous medium has been reported elsewhere [25]. After printing a two-layer line trace of the SWCNTs/SSDNA, Pd alkanethiolate electrodes were printed to form electrical contact pads to both ends of the SWCNT network. $I(V)$ measurements revealed the conducting nature of the randomly interconnected SWCNTs/SSDNA to behave linearly [6]. With the known dimensions of the pattern, the corresponding resistivity of the composite was $1.14 \times 10^{-3} \Omega\text{m}$ [6].

Coalescence Between Two Drops on a Non-porous Substrate: Models and Observations

A building block to understanding the effects of coalescence on inkjet printed films is understanding coalescence between two drops on a non-porous substrate. Multiple recent investigations have been conducted within the past decade to better understand this phenomenon [16–18].

Li et al. [16] conducted an experimental study on the evolution of the spread length (i.e. the length of the two coalesced drops along their original centers) of a falling drop coalesced with a stationary sessile drop. They examined two coalescing water droplets and two coalescing ethylene glycol drops on polished steel. In both cases, they kept the volume of the two drops equal and varied their center-to-center spacing. They then used their observations to establish correlation equations to determine deposition conditions for forming continuous or discontinuous coalesced lines. Casterjón-Pita et al. [17] conducted experiments and numerical simulations to investigate a falling drop coalescing with a stationary sessile drop. Their study considered two coalescing glycerol/water drops seeded with TiO_2 particles on a polymethyl methacrylate (Perspex, Lucite) substrate. The drop

volume was held constant in all experiments while the drop spacing was varied. They used a lattice Boltzmann method including a model for contact angle hysteresis in order to describe the internal flows and the evolution of the spread length during the coalescence event. Their experimental results were obtained using a high speed camera, particle image velocimetry, and image processing algorithms. Comparisons showed qualitative agreement but quantitative discrepancies. Most recently, Yang et al. [18] conducted an experimental investigation of the coalescence between two consecutively printed drops of a colloidal mixture of carboxylate-modified polystyrene fluorescent beads in deionized (DI) water on cleaned glass substrates. Varying the center-to-center spacing and the deposition time difference between the two drops, they studied the morphology of the composite drop. The deposition time difference was varied from 0.2s (well after the first drop had equilibrated on the surface) until 0.9s (about 60% of the time for the first drop to evaporate). Using a fluorescent microscope, they obtained a measurement of particle density in the dried composite drop. Their results showed that the contact line of the first drop remained pinned throughout the entire evaporation and coalescence processes, the relaxation time of the water-air interface of the merged drop was smaller than that of a single drop on a dry surface, and the circularity of the composite drop decreases with increased drop spacing for all jetting delays. Moreover, due to capillary forces and inertia, they observed that the suspended particles in the second drop flow toward the first drop resulting in more particles deposited on the first drop side, a phenomenon referred to as drawback. Throughout their experiments, the initial volumes of the two coalescing drops were equal and the drop spacings either were or were assumed to be as prescribed.

Contributions of the Current Study

Although great progress has been made in the recent coalescence studies on a non-porous substrates, there are still a few issues to be addressed in the context of functional printing. The literature on coalescence between two consecutively deposited drops is limited on the variety of ink/substrate systems, with none of the inks containing functional material and all of the ink/substrate systems being partially wetting. Different ink/substrate systems can generate very different results depending on the wettability and the contact angle hysteresis of the ink/substrate system. Furthermore, the path from coalescence to functional performance was not explored.

The contributions of this study are as follows.

1. The printing platform is a functional ink containing Palladium hexadecanethiolate, a material proven useful for facile fabrication of metallic interconnects, surface-enhanced Raman scattering substrates, and Hydrogen gas sensing [6, 26–28].
2. The ink used in this study has a relatively high vapor pressure at room temperature and the ink/substrate used exhibits small contact angle hysteresis [29].
3. Experiments are conducted in order to track ink migration after the coalescence process for two consecutively printed adjacent drops with their deposition time difference varying throughout the entire lifetime of the first drop.

- Building upon the two-drop experiments, lines with varying drop spacing and deposition time difference are printed and their optical uniformity and functional performance are compared.

Experimental Details

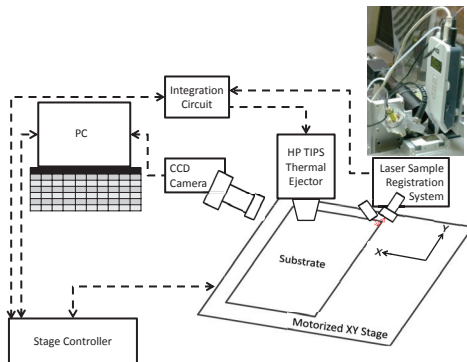


Figure 3. Schematic and optical image (inset) of inkjet functionalization system used. Dotted lines indicate signal/information flow.

Inkjet System

The inkjet system used for conducting experiments for this study is shown in Figure 3. The motion system consists of an XY stage (Anorad-XY-C-150-AAA0), which uses DC servo driven permanent magnet epoxy core linear motors for independent motion in both axes. The motion is controlled by a SPiiPlus Series Stand Alone controller, with linear encoder feedback of $0.5\mu\text{m}$. The print-head standoff distance was held constant at approximately $250\mu\text{m}$ from the substrates in all experiments. The standoff distance between the print-head and the substrates was controlled using a manual z-axis adjustment stage (Edmund R-56-335). The drop ejection system used is provided by HP[®], utilizes thermal inkjet technology, and offers print-heads with 10, 12, or 16 nozzles. The nozzle orifices range from $8.0\mu\text{m}$ to $80.0\mu\text{m}$. The print-head used for all experiments consists of 12 nozzles with a nominal orifice diameter of $67\mu\text{m}$. The system also includes a Sony[®] XC-ST50 charged coupled device (CCD) camera for viewing during deposition and a laser sample registration system for mapping out edges of a substrate [30].

Materials

The ink platform used in these experiments is an 32mM solution of Pd hexadecanethiolate ($\text{Pd}(\text{SC}_{16}\text{H}_{35})_2$) dissolved in toluene. The ink was prepared by mixing an equimolar ratio of Pd acetate and hexadecyl alkanethiol. Following the reaction, the solution became viscous, and the yellow color deepened to orange-yellow [31] indicating that $\text{Pd}(\text{SC}_{16}\text{H}_{35})_2$ had formed. The $\text{Pd}(\text{SC}_{16}\text{H}_{35})_2$ was then dissolved in toluene to make specified concentration (32mM).

The substrates employed in this study were pure silicon (Si) wafers and oxidized silicon (SiO_2/Si) wafers. The polished, coinrolled Si wafers were received from Nova Electronic Materials, Inc. (Item ID STK9281). Prior to printing, both the SiO_2/Si and

Si wafers were cleaned in a sonication bath (Brandson 2510) for 5 min in acetone followed by 5 min in isopropanol. The wafers were blown dry subsequently by compressed air.

Instruments for Measurement and Processing

Bright field images were captured using an Olympus optical microscope system (Olympus bx51 microscope, dp70 CCD camera, th4-100 lamp, 10X zoom, and 1/550 sec exposure) for determining ink migration between two consecutively printed drops. For the printed line experiments, an Olympus BX-60 optical microscope system was used to obtain bright field images. Thermolysis of the printed lines was carried out using a hot plate at 250°C . Electrical characterization of the thermolyzed lines was performed utilizing a semiconductor characterization system (SCS) (Keithley 4200 SCS) and four-probe station with light tight enclosure (LTE) (Micromanipulator 7000 LTE). Current vs. voltage (IV) plots were generated by applying a voltage sweep between two contacts on either side of the printed line. The voltage was swept from -5.0 to 5.0 V with step size of 0.1 V and the resistance between the two contact points was taken as the average value of voltage/current at each respective data point. The ambient temperature during the printing experiments was observed using a K type thermocouple and was held constant at $23.0^\circ \pm 2\%$.

Results and Discussion

Proxy for Determining Ink Migration

An experiment was conducted to validate the use of an index of contrast to serve as a proxy for the amount of deposited functional material. Nine arrays of 40 drops were printed onto an Si wafer, each array corresponding to a different number of layers (1-9). The printed arrays were then imaged via optical microscope. These resulting color images were then converted to grayscale images via MATLAB. Image segmentation was then conducted by applying MATLAB's image processing toolbox to the grayscale images to extract all printed drops. Next, the mass proxy (MP) was calculated using an index of contrast for each drop written as

$$MP = \sum_{i,j \in S} H(R_{ij} - R_S) (R_S - R_{ij}), \quad (1)$$

where $H(z)$ is the Heaviside step function that is 0 for all $z \leq 0$ and 1 otherwise, R_{ij} is the grayscale value of the pixel in the i th row and j th column of the image ($R_{ij} = 255$ corresponds to white while $R_{ij} = 0$ corresponds to black), S is the set of all image pixels within a given drop, and R_S is the minimum grayscale value of the substrate. The results, displayed in Figure 4, show that Equation (1) exhibits an exponential behavior and reaches saturation between 4 and 5 layers. On the other hand, Equation (1) has a linear regime between 0 and ≈ 2 layers, even more so as the number of layers approaches 1. Therefore, since Equation (1) is only being used in this study for layers between 0 and ≈ 1 , the region exhibiting a linear behavior, this method for sensing solute mass deposition for single drops and double drops is valid.

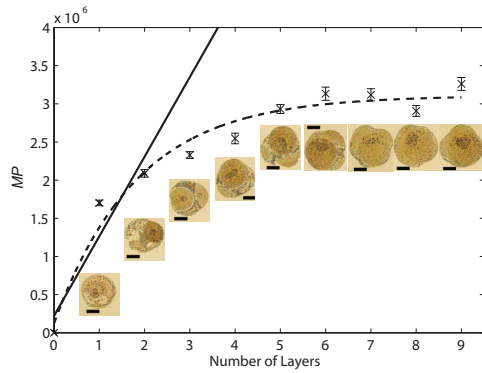


Figure 4. Plot demonstrating the validity of using MP as a proxy for deposited solute mass. Exponential fit (dotted line curve) calculated using least squares. Linear fit is through 0-2 layers. Each inset is a representative image vertically aligned with its corresponding number of layers. Scale bars are $50\mu\text{m}$ in length. Errorbars represent 95% confidence intervals.

Two-Drop Experiments

Figures 5 and 6 show the highlights of the experimental process for the two-drop experiments. Multiple pairs of drops (≥ 85 pairs) were printed onto a Si wafer with a fixed nominal spacing ($80\mu\text{m}$) in the print-head scan direction (X-direction) and the deposition time difference was varied from 25ms to 400ms. Optical micrographs were then taken for the use of image analysis to calculate the ink migration from the first deposited drop (the drop located on the left side of each pair in Figure 6) to the second deposited drop (the drop located on the right side of each dyad in Figure 6).

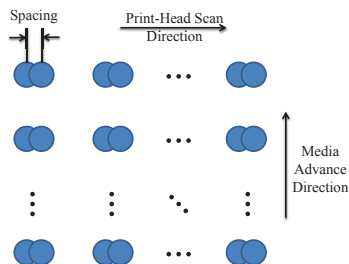


Figure 5. Schematic of print pattern two-drop experiments.

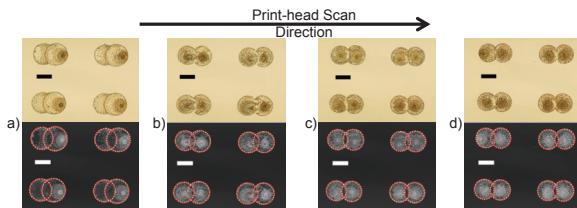


Figure 6. Adjacent printed pairs of drops with a nominal spacing of $80\mu\text{m}$ and a deposition time difference of a) 75ms b) 175ms c) 275ms and d) 325ms. Top Row: raw images. Bottom Row: corresponding negative grayscale images illustrate process employed to quantify amount of ink migration with circular borders (dotted (red) line) superimposed onto each drop. Scale bars are $100\mu\text{m}$ in length.

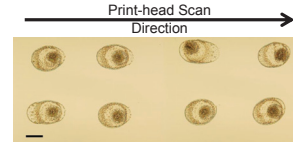


Figure 7. Adjacent printed pairs of drops (some exhibiting drawback) with an $80\mu\text{m}$ nominal spacing and 25ms deposition time difference. Scale bar is $100\mu\text{m}$ in length.

Image analysis was conducted via MATLAB's image processing toolbox in order to find the amount of solute migration from the first drop to the second drop. The optical micrographs were first converted to grayscale images using MATLAB's image analysis toolbox. Next, circular borders for each drop within each dyad were found using MATLAB's *imfindcircles* function. The percent of solute migration (psm) from the first drop to the second drop was then computed for each pair by

$$psm = \frac{MP_2 - MP_1}{2\overline{MP}}, \quad (2)$$

where MP_1 and MP_2 are the mass proxies computed using Equation (1) for the first and second drops, respectively, and \overline{MP} is the average mass proxy for a single drop. The results of this process are shown in Figure 8. The data gathered for 25ms is not shown because the image analysis method could not distinguish more than one drop for each dyad. However, it can be qualitatively observed from the printed dyads in Figure 7 that some of the drops displayed a negative psm (i.e. solute tended to migrate from the second drop into the first drop), which is in agreement with what has been observed in the literature when the contact line of the first drop is pinned [11, 12, 18, 20].

The temporal trend is that solute migration from the first drop into the second drop initially increases until reaching a maximum at 100ms, after which it decreases exponentially until reaching 0% around 325ms. This trend can be explained by means of surface energy in addition the contact line pinning forces acting on the first drop. At deposition time differences less than or equal to 25ms the ink appears to flow from the second drop into the first drop. This is as expected since, everything else equal, the first drop has a higher surface energy due to its higher surface area. This result is also in agreement with the work of Weon and Je for spherical bubbles and drops [32]. However, as the first drop evaporates, the solute concentration at the contact line increases due to capillary flow, which results in an increased a Marangoni flow in the direction of the second drop. This result is similar to the observations of Karpitschka and Riegler [33]. The momentum continues to increase in the direction of the second drop until the contact line pinning force on the first drop becomes a minimum, corresponding to the when the value of the contact angle of the first drop reaches that of its receding contact angle, most likely occurring around 100ms in accordance with Figure 8. As the drop detaches from the coffee ring, the surface tension at the contact line quickly stabilizes, resulting in the observed fast decrease in ink migration from the first drop into the second drop. From there it slowly decreases to until there is no more liquid left in the first drop, leaving no chance of drop coalescence and therefore, no mechanism for solute transport.

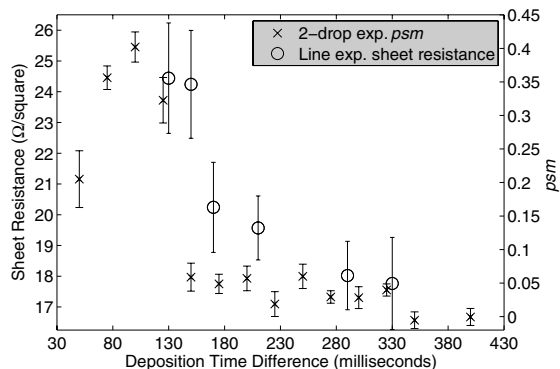


Figure 8. Estimated percent of solute migration from first drop to the second drop in the two-drop experiment (x's) with Measured sheet resistance from printed line experiment (o's). Error bars reflect 95% confidence intervals.

Printed Line Experiments

Further experiments were conducted for printed single-layer lines with varied drop spacing and varied delay between deposition of adjacently located drops. Qualitatively it appears that maximum ink migration occurs at a delay of 50ms. After depinning the composite drop will have a net velocity in the direction of the second drop. Therefore, the composite drop is expected to gain velocity in the print-head scan direction with each subsequently printed drop, until becoming balanced by viscous forces and inertia, which increase with increased speed and contact area.

Further observing, the lines printed with small delays (at 5ms) seem to be somewhat uniform with the exceptions of aggregates of solute riddled throughout the center of the line and thinner areas located toward the ends of the line. The random aggregates riddled throughout the middle section of these lines may come from the small delays being similar to the prolonged [14, 15] time required for the composite drop to settle after the coalescence event. The thinner areas located toward the ends of the lines printed with a delay of 5ms are indicative of the contact line slipping at the ends of the lines, which is expected. During the printing process the contact angle at the site of the first drop decreases to its receding contact angle while the film on the process side approaches the advancing contact angle. This gives a result of the contact line slipping on the side where the first drop was deposited. Once printing has ceased, the traveling wave occurring within the coalesced film moves away from the process direction causing the contact angle on the process side to decrease and eventually slip. Furthermore, the large slope at the end points implies that this is where mass flux is the largest. In addition, the ends are farthest from neighboring liquid molecules, making it difficult for escaping vapor molecules to return back to the liquid reservoir (the coalesced liquid line). Furthermore, this makes it difficult for the liquid from the bulk of the line to flow to the ends fast enough to keep the contact line pinned. In all cases, uniformity of the printed line increases as the delay increases, which is in agreement with the two-drop experiment.

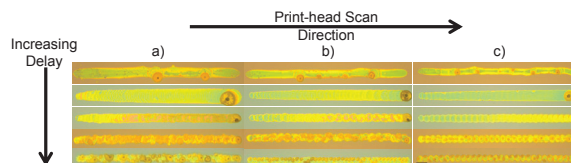


Figure 9. Printed line morphologies with a) a drop pitch of $40\mu\text{m}$ and a delay of 5ms, 50ms, 100ms, 200ms, and 290ms; b) a drop pitch of $70\mu\text{m}$ and a delay of 5ms, 70ms, 100ms, 200ms, and 290ms; c) a drop pitch of $100\mu\text{m}$ and a delay of 5ms, 50ms, 100ms, 200ms, and 290ms. Scale bars are $200\mu\text{m}$ in length.

Additional experiments were conducted to see how coalescence translates from ink migration to functional performance. Several lines of the functional ink were printed, each containing ten layers with a nominal drop spacing of $40\mu\text{m}$. For each line, the deposition time difference between adjacently printed drops was set to a different value. The sheet resistance for each line was obtained by using the measured resistances in conjunction with the probe spacing and line width gathered from optical micrographs. The probe spacing was deduced from the indentations left behind during the electrical measurements. For comparison, the resulting sheet resistances are plotted on the same graph as the ink migration experiments in Figure 8. As evident from Figure 8, the resulting functional performance follows a trend identical to that of the ink migration with a subtle shift right. This shift is as expected, since the drop spacing is smaller for the printed lines, thus requiring more time to elapse to reduce the occurrence of ink migration. Lines were printed with smaller deposition time differences than shown. However, no measurable current could be passed through them due to ink migration.

Conclusions

Avoiding coalescence between adjacently printed drops can eliminate ink migration between drops, relax minimum print speeds and drop ejection frequencies, avoid additional printing time associated with reduced line-to-line spacing, reduce the coffee ring effect from the scale of the entire film to that of individual drops. This study has investigated the occurrence of coalescence between adjacently printed drops of a functional ink containing a high vapor pressure solvent onto non-porous Si and SiO_2 substrates. Qualitative descriptions of the momenta acting on the first printed drop are used to explain the effects. The main contributing factors to the ink migration are thought to be differences in surface energy between the two drops as well as the depinning of the contact line. Image analysis-based measurements were proposed and experimentally validated in order to describe solute mass migration between two adjacently printed drops.

References

- [1] Calvert, P., 2001. "Inkjet printing for materials and devices". *Chemistry of Materials*, **13**(10), Oct, pp. 3299–3305.
- [2] Shimoda, T., Morii, K., Seki, S., and Kiguchi, H., 2003. "Inkjet printing of light-emitting polymer displays". *MRS Bulletin*, **28**(11), Nov, pp. 821–827.
- [3] de Gans, B., Duineveld, P., and Schubert, U., 2004. "Inkjet printing

- of polymers: State of the art and future developments". *Advanced Materials*, **16**(3), Feb 3, pp. 203–213.
- [4] Burns, S., Cain, P., Mills, J., Wang, J., and Sirringhaus, H., 2003. "Inkjet printing of polymer thin-film transistor circuits". *MRS Bulletin*, **28**(11), Nov, pp. 829–834.
- [5] Subramanian, V., Chang, P., Lee, J., Molesa, S., and Volkman, S., 2005. "Printed organic transistors for ultra-low-cost RFID applications". *IEEE Transactions on Components and Packaging Technologies*, **28**(4), Dec, pp. 742–747. 10th Thermionic Workshop, Sophia Antipolis, France, Sep 29-Oct 01, 2004.
- [6] Bhuvana, T., Boley, W., Radha, B., Dolash, B. D., Chiu, G., Bergstrom, D., Reifengerger, R., Fisher, T. S., and Kulkarni, G. U., 2010. "Inkjet printing of palladium alkanethiolates for facile fabrication of metal interconnects and surface-enhanced Raman scattering substrates". *Micro & Nano Letters*, **5**(5), Oct, pp. 296–299.
- [7] Singh, M., Haverinen, H. M., Dhagat, P., and Jabbour, G. E., 2010. "Inkjet Printing-Process and Its Applications". *Advanced Materials*, **22**(6), Feb 9, pp. 673–685.
- [8] Kumar, V., Boley, J. W., Yang, Y., Ekowaluyo, H., Miller, J. K., Chiu, G. T. C., and Rhoads, J. F., 2011. "Bifurcation-based mass sensing using piezoelectrically-actuated microcantilevers". *Applied Physics Letters*, **98**(15), Apr 11.
- [9] Derby, B., and Reis, N., 2003. "Inkjet printing of highly loaded particulate suspensions". *MRS Bulletin*, **28**(11), Nov, pp. 815–818.
- [10] Derby, B., 2008. "Bioprinting: inkjet printing proteins and hybrid cell-containing materials and structures". *Journal of Materials Chemistry*, **18**(47), pp. 5717–5721.
- [11] Stringer, J., and Derby, B., 2010. "Formation and Stability of Lines Produced by Inkjet Printing". *Langmuir*, **26**(12), Jun 15, pp. 10365–10372.
- [12] Soltman, D., Smith, B., Kang, H., Morris, S. J. S., and Subramanian, V., 2010. "Methodology for Inkjet Printing of Partially Wetting Films". *Langmuir*, **26**(19), Oct 5, pp. 15686–15693.
- [13] Boley, W., Bhuvana, T., Hines, B., Sayer, R. A., Chiu, G., Fisher, T. S., Bergstrom, D., Reifengerger, R., and Kulkarni, G. U., 2009. "Inkjet Printing Involving Palladium Alkanethiolates and Carbon Nanotubes Functionalized with Single-Strand DNA". In NIP 25: Digital Fabrication 2009, Technical Program and Proceedings, Soc Imaging Sci & Technol; Imaging Soc Japan, pp. 824–827. 25th International Conference on Digital Printing Technologies, Louisville, KY, Sep 20-24, 2009.
- [14] Andrieu, C., Beysens, D., Nikolayev, V., and Pomeau, Y., 2002. "Coalescence of sessile drops". *Journal of Fluid Mechanics*, **453**, Feb 25, pp. 427–438.
- [15] Gokhale, S., DasGupta, S., Plawsky, J., and Wayner, P., 2004. "Reflectivity-based evaluation of the coalescence of two condensing drops and shape evolution of the coalesced drop". *Physical Review E*, **70**(5, Part 1), Nov.
- [16] Li, R., Ashgriz, N., Chandra, S., Andrews, J. R., and Drappel, S., 2010. "Coalescence of two droplets impacting a solid surface". *Experiments in Fluids*, **48**(6), Jun, pp. 1025–1035.
- [17] Castrejon-Pita, J. R., Betton, E. S., Kubiak, K. J., Wilson, M. C. T., and Hutchings, I. M., 2011. "The dynamics of the impact and coalescence of droplets on a solid surface". *Biomicrofluids*, **5**(1), Mar.
- [18] Yang, X., Chhasatia, V. H., Shah, J., and Sun, Y., 2012. "Coalescence, evaporation and particle deposition of consecutively printed colloidal drops". *Soft matter*, **8**(35), pp. 9205–9213.
- [19] Wu, J.-T., Hsu, S. L.-C., Tsai, M.-H., Liu, Y.-F., and Hwang, W.-S., 2012. "Direct ink-jet printing of silver nitrate-silver nanowire hybrid inks to fabricate silver conductive lines". *Journal of Materials Chemistry*, **22**(31), pp. 15599–15605.
- [20] Duineveld, P., 2003. "The stability of ink-jet printed lines of liquid with zero receding contact angle on a homogeneous substrate". *Journal of Fluid Mechanics*, **477**, Feb 25, pp. 175–200.
- [21] Hu, H., and Larson, R., 2002. "Evaporation of a sessile droplet on a substrate". *Journal of Physical Chemistry B*, **106**(6), Feb 14, pp. 1334–1344.
- [22] Deegan, R., Bakajin, O., Dupont, T., Huber, G., Nagel, S., and Wittent, T., 1997. "Capillary flow as the cause of ring stains from dried liquid drops". *Nature*, **389**(6653), Oct 23, pp. 827–829.
- [23] Tekin, E., de Gans, B., and Schubert, U., 2004. "Ink-jet printing of polymers - from single dots to thin film libraries". *Journal of Materials Chemistry*, **14**(17), pp. 2627–2632.
- [24] Yunker, P. J., Still, T., Lohr, M. A., and Yodh, A., 2011. "Suppression of the coffee-ring effect by shape-dependent capillary interactions". *Nature*, **476**(7360), Aug 18, pp. 308–311.
- [25] Lahiji, R. R., Dolash, B. D., Bergstrom, D. E., and Reifengerger, R., 2007. "Oligodeoxyribonucleotide association with single-walled carbon nanotubes studied by SPM". *Small*, **3**(11), Nov, pp. 1912–1920.
- [26] Bhuvana, T., and Kulkarni, G. U., 2008. "Highly conducting patterned Pd nanowires by direct-write electron beam lithography". *ACS Nano*, **2**(3), Mar, pp. 457–462.
- [27] Bhuvana, T., and Kulkarni, G. U., 2008. "A SERS-activated nanocrystalline Pd substrate and its nanopatterning leading to biochip fabrication". *Small*, **4**(5), May, pp. 670–676.
- [28] Sagade, A. A., Radha, B., and Kulkarni, G. U., 2010. "Intricate nature of Pd nanocrystal-hydrogen interaction investigated using thermolysed Pd hexadecylthiolate films". *Sensors and Actuators B-Chemical*, **149**(2), Aug 19, pp. 345–351.
- [29] Boley, J. W., 2013. "Print mask design for inkjet functional printing". PhD thesis, Purdue University, May.
- [30] Post, N. J., 2007. "Precision micro-deposition of functional layers using inkjet drop-on-demand and applications to the functionalization of microcantilever sensors". Master's thesis, Purdue University, August.
- [31] Thomas, P., Lavanya, A., Sabareesh, V., and Kulkarni, G., 2001. "Self-assembling bilayers of palladiumthiolates in organic media". *Proceedings of the Indian Academy of Sciences-Chemical Sciences*, **113**(5-6), Oct-Dec, pp. 611–619.
- [32] Weon, B. M., and Je, J. H., 2012. "Coalescence Preference Depends on Size Inequality". *Physical Review Letters*, **108**(21), May 29.
- [33] Karpitschka, S., and Riegler, H., 2012. "Noncoalescence of Sessile Drops from Different but Miscible Liquids: Hydrodynamic Analysis of the Twin Drop Contour as a Self-Stabilizing Traveling Wave". *Physical Review Letters*, **109**(6), Aug 10.

Author Biography

Dr. Boley received a Bachelor of Science in Mechanical Engineering with a double major in Mathematics from The University of Kentucky in Lexington, KY in May 2006. He continued his studies at The University of Kentucky and earned a Master of Science in Mechanical Engineering in August 2007. Dr. Boley recently received a Ph.D. in May 2013 from the School of Mechanical Engineering at Purdue University in West Lafayette, IN, specializing in inkjet functional printing. He currently holds a post-doctoral position in the School of Mechanical Engineering at Purdue University.